Passive interferometric imaging for limited illumination using slowness diagnosis and directionally constrained Gaussian Beam Migration

Carlos Almagro Vidal, Joost van der Neut, Deyan Draganov, Kees Wapenaar (Delft University of Technology) and Arie Verdel (TNO Utrecht and Delft University of Technology)*

SUMMARY

With seismic interferometry, the subsurface reflection response can be retrieved from recordings of passive sources that are located relatively deep in the subsurface. The retrieved data can be used to image subsurface structures. Succesful interferometric imaging relies upon the availability of passive records from sufficient passive sources in the subsurface that illuminate the receivers from all angles. Such a condition would be difficult to meet in practical applications. Incomplete passive-source distributions would result in the retrieval of inaccurate Green's functions containing artefacts that can disturb the interferometric imaging process. We propose an alternative imaging method for passive data based on Gaussian beams. In this method, passive gathers are cross-correlated individually. The dominant radiation direction of each virtual source in each correlated gather is estimated. The correlated gathers are imaged indivually, using an adapted migration algorithm that takes the dominant virtual source radiation direction into account. In this way, correct partial subsurface images can be constructed even from a limited number of passive sources.

INTRODUCTION

Seismic interferometry (SI) aims to reconstruct the impulse response between receivers, with a virtual source located at one of them. To accomplish this, it is required to have passive sources illuminating the receivers uniformly from all possible angles. An example of SI applied to passive seismics can be seen in Draganov et al. (2006) and Draganov et al. (2010). The authors applied crosscorrelation to retrieve virtual-source records, which were consecutively migrated. The migration of correlated data has been referred to as interferometric imaging (II) (Schuster et al., 2004). Nowack et al. (2006) showed another example of II, this time carried out using slant-stack windows of the data, and migrating the autocorrelated data by means of Gaussian beams.

In Figure 1 we illustrate the process of retrieving a reflection response between two receivers. The specular ray from the passive source (the direct arrival to the first receiver) defines the direction in which the correct reflection ray can be found. For each passive source - virtual source pair, there is a unique ray-parameter that defines this specular ray. We will make use of this knowledge by using only this ray-parameter during II.

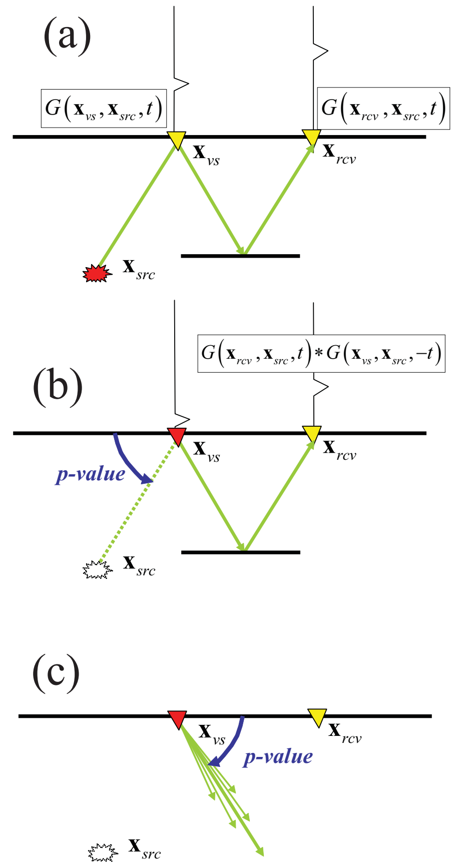

Figure 1: *Illustration of passive seismic interferometry. (a) A receiver at $\mathbf{x}_{rcv}$ records a field originating from a subsurface source ($\mathbf{x}_{src}$) after being scattered by a reflector. A receiver at $\mathbf{x}_{vs}$ records the direct field from the source. The source is along the specular ray passing through the receivers. (b) The cross-correlation of the response at $\mathbf{x}_{rcv}$ with the one at $\mathbf{x}_{vs}$ would retrieve the reflection response at $\mathbf{x}_{rcv}$ as if a virtual source (vs) was located at receiver $\mathbf{x}_{vs}$. The locations of the source and virtual source define a unique ray-parameter (p-value). (c) The value of this ray-parameter defines the direction in which the reflector is to be located with respect to the virtual source. Only this ray-parameter is needed, not the location of the passive source $\mathbf{x}_{src}$, to find the desired stationary-phase region.*

MIGRATION SCHEME

For transient sources, Wapenaar and Fokkema (2006) introduce a relation to retrieve the Green's function $G(\mathbf{x}_{rcv},\mathbf{x}_{vs},\omega)$ between a receiver at $\mathbf{x}_{rcv}$ and a virtual source at $\mathbf{x}_{vs}$ from recordings at these two points:

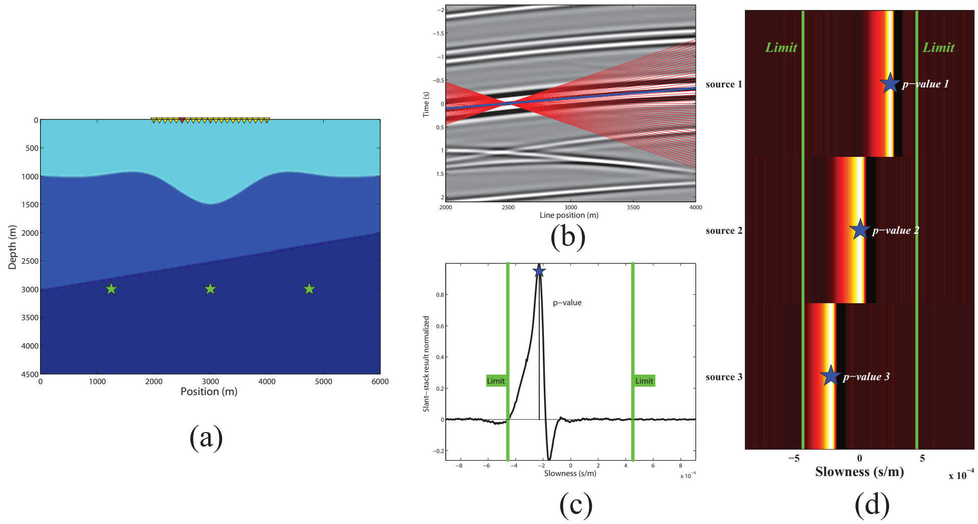

Figure 2: ***(a)*** *Synthetic model, with a 41-receiver array at the surface (yellow triangles) and 3 sources in the subsurface (green stars).* ***(b)*** *correlated panel, from source at 4750 m in model in figure 2a, around the virtual-source function (time=0 s) located at 2500 m (red triangle in (a)). The red lines indicate slownesses for which ray-parameter analysis is carried out (See Almagro Vidal et al. (2011).* ***(c)*** *The slowness-distribution diagram for (b). The blue star denotes the dominant ray-parameter (p-value) from the incident field of the source located at 4750 m.* ***(d)*** *The illumination diagram (slowness distribution) for the correlated panels from each of the three subsurface sources in (a), with their dominant ray-parameter (p-value).*

$$2\Re\left\{\hat{G}\left(\mathbf{x}_{rcv},\mathbf{x}_{vs},\omega\right)\right\}\hat{S}_0 \propto \sum_i \hat{C}_i\left(\mathbf{x}_{rcv},\mathbf{x}_{vs},\mathbf{x}_{src}^{(i)},\omega\right), \quad (1)$$

where $\Re$ stands for real part and ω is the angular frequency; $\hat{C}_i\left(\mathbf{x}_{rcv},\mathbf{x}_{vs},\mathbf{x}_{src}^{i},\omega\right)$ is the correlation function of a single passive source at $\mathbf{x}_{src}^{(i)}$, described as follows:

$$\hat{C}_i\left(\mathbf{x}_{rcv},\mathbf{x}_{vs},\mathbf{x}_{src}^{(i)},\omega\right) = \hat{P}\left(\mathbf{x}_{rcv},\mathbf{x}_{src}^{(i)},\omega\right)\hat{P}^*\left(\mathbf{x}_{vs},\mathbf{x}_{src}^{(i)},\omega\right), \quad (2)$$

where asterisk denotes complex conjugation; $\hat{P}(\mathbf{x}_{rcv},\mathbf{x}_{src}^{(i)};\omega)$ and $\hat{P}(\mathbf{x}_{vs},\mathbf{x}_{src}^{(i)};\omega)$ stand for the records at $\mathbf{x}_{rcv}$ and $\mathbf{x}_{vs}$, respectively, due to a source at $\mathbf{x}_{src}^{(i)}$.

Almagro Vidal et al. (2011) introduced a method to determine the dominant ray-parameter of a correlated gather at a specific virtual source location. An illustration of this method is provided in Figures 2a-c. The aim of the method was to separate shot records which are dominated by surface waves from those responsible for the retrieval of reflections. Quantification analysis of the ray-parameters also results in an illumination diagram by source panel (Figure 2d). As mentioned before, the dominant ray-parameter defines the specular ray with respect to the virtual-source location.

Since from the cross-correlation we obtain correct reflections for this specific certain ray-parameter only, we require a directionally constrained migration scheme. The method we proposed here is derived from the work of Popov et al. (2010), where the imaging condition is defined by the correlation of a forward wavefield with the backprojection of the recorded field; both fields are reconstructed using Gaussian beams, which is in essence a high-frequency technique with the advantage of approximating the wavefield closely when adding the beams together. For the passive-seismic case with isotropic illumination, the full forward impulse response should be used for migration. For partial migration of the correlation function $C_i(x_{rcv},x_{vs},x_{src}^{(i)},t)$ of a single source, it may be better to reduce the forward field to a single ray-parameter.

In Popov et al. (2010), the Green's function is represented as a summation over Gaussian beams, u_{GB}, propagating into different directions. This is represented by:

$$G_{GB}(\mathbf{x},\mathbf{x}_0,\omega) = \int_0^{\pi}\int_0^{2\pi} \Phi(\theta,\phi,\omega)\ u_{GB}(s,\overline{n},\theta,\phi,\omega)d\theta d\phi, \quad (3)$$

where Φ are the initial amplitudes of the Gaussian beams. The Green's function representation from a source point $\mathbf{x_0}$ is here given as the summation of Gaussian beams taking the impulse response u_{GB} in ray coordinates s and $\overline{n}$ (following *Červený* et al. (1982)), and integrating over the azimutal and polar angles θ and ϕ, they create the Green's function as a Gaussian beam summation.

Using the results from the illumination diagnosis previously described (Almagro Vidal et al. (2011)), to enhance the illumination derived from the direct arrivals, the forward field is simplified for a single angle, defined by the dominant p-value

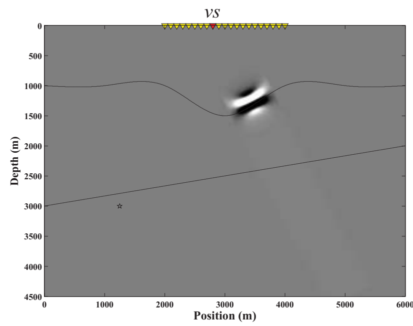

(a) Beam projection of the forward field.

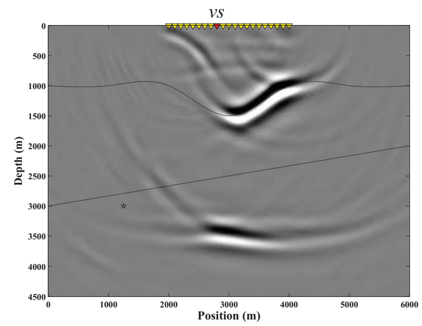

(b) Backprojected cross-correlation at the virtual source position.

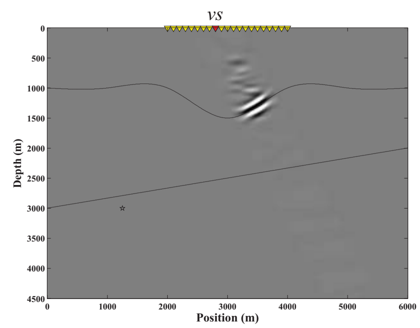

(c) Result from imaging condition.

Figure 3: *Results from the model in Figure 2a, with passive source at 1250 m and virtual source located at 2800 m (red receiver), and imaging condition at instant 0.68 s:* ***(a)*** *Forward field focused at a single direction from the virtual-source location.* ***(b)*** *Backprojection of the cross-correlation.* ***(c)*** *Imaging condition.*

in the source function acting in the cross-correlation product. Therefore, the Green's function of a source located at $\mathbf{x_0}$ evaluated at $\mathbf{x}$ is now constrained by the p-value, and is represented then as $G_{GB}(p, \mathbf{x}, \mathbf{x}_0, \omega)$.

The forward wavefield generated at the virtual source position ($B_i^{\Downarrow}$, figure 3a) is constructed using this asymptotic form of the Green's function with the source location $\mathbf{x}_{src}^{(i)}$ using as source point the location of the virtual source x_{vs}. Both locations determine the p_i-value:

$$B_i^{\Downarrow}(p_i, \mathbf{x}, \mathbf{x}_{vs}, t) \approx \frac{1}{\pi} \Re \int_0^{\infty} G_{GB}(p_i, \mathbf{x}, \mathbf{x}_{vs}, \omega)\, S_f(\omega)\, e^{-i\omega t}\, d\omega, \tag{4}$$

where $S_f(\omega)$ is the frequency spectrum from the cross-correlation result. For the backprojection of the recorded field ($U_i^{\Uparrow}$, figure 3b), we build the asymptotic form of the Green's function at certain instant t_0:

$$G_{GB}(\mathbf{x}, \mathbf{x}_{rcv}, t, t_0) = \frac{1}{\pi} \Re \int_0^{\infty} G_{GB}(\mathbf{x}, \mathbf{x}_{rcv}, \omega)\, e^{-i\omega(t-t_0)}\, d\omega. \tag{5}$$

Now from the cross-correlation result $C_i(x_{rcv}, x_{vs}, x_{src}^{(i)}, t)$ of the recordings of a single event i for each virtual-shot position, we reconstruct the backprojection of the cross-correlation result:

$$\begin{aligned} &U_i^{\Uparrow}(\mathbf{x}, \mathbf{x}_{vs}, t_0) \\ &\approx -2 \int_{t_0}^{T} \int_{\mathbf{x}_{rcv}} C_i(\mathbf{x}_{rcv}, \mathbf{x}_{vs}, \mathbf{x}_{src}^{(i)}, t)\, \frac{\partial}{\partial z}\, G_{GB}(\mathbf{x}, \mathbf{x}_{rcv}, t, t_0) d\mathbf{x}_{rcv} dt. \end{aligned} \tag{6}$$

The two terms $B_i^{\Downarrow}$ and $U_i^{\Uparrow}$ set the imaging condition under the zero-time-lag correlation function W_i (figure 3c):

$$W_i(p_i, \mathbf{x}, \mathbf{x}_{vs}) = \int_{t_0}^{T} B_i^{\Downarrow}(p_i, \mathbf{x}, \mathbf{x}_{vs}, t)\, U_i^{\Uparrow}(\mathbf{x}, \mathbf{x}_{vs}, t)\, dt. \tag{7}$$

The partial image W_i describes for which ray-parameter the image is defined. With all passive sources available, stacking the individual partial images over i should give the desired total image of the subsurface. However, with scarce passive sources, already the evaluation of only one source i, the partial image may give an acceptable result.

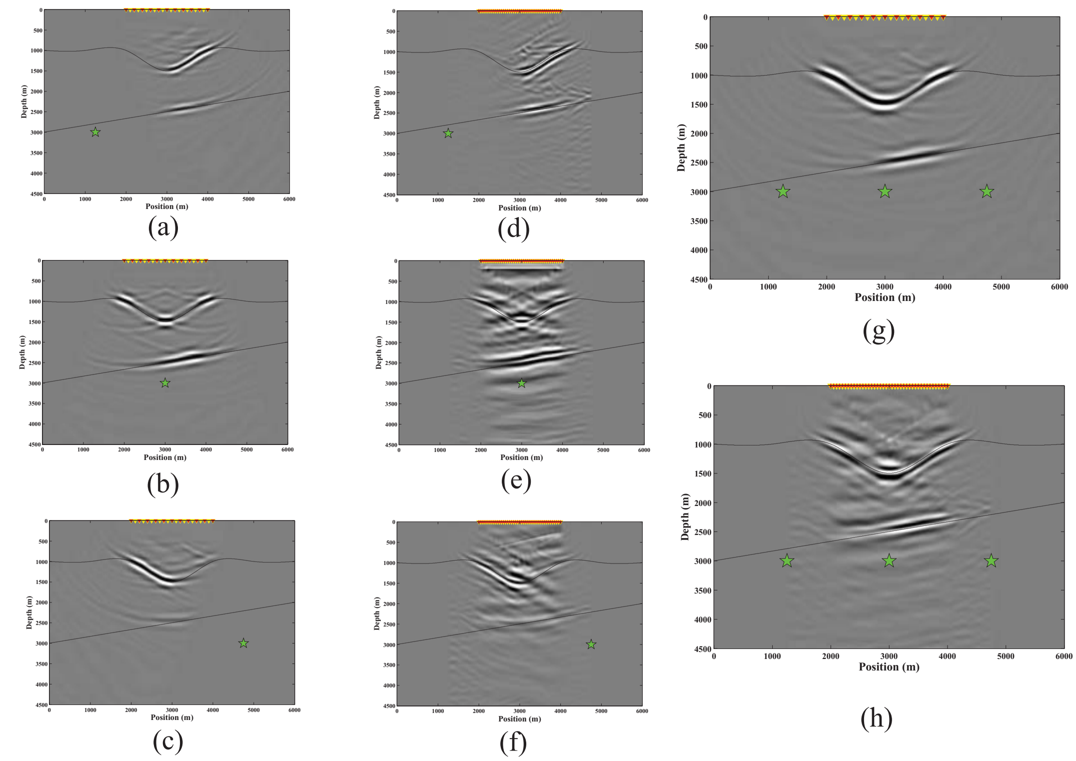

Figure 4: *Migrated images of the subsurface for the model in Figure 2a obtained for subsurface-source position indicated by the green stars:* ***(a)**, **(b)** and **(c)**, Images obtained from p-evaluation followed by directionally constrained Gaussian beam migration.* ***(d)**, **(e)** and **(f)**, Images from a conventional interferometric imaging scheme.* ***(g)** Passive inteferometry imaging result, summing (a), (b) and (c).* ***(h)** seismic interferometry imaging result, migrating virtual-shot records from sequential cross-correlation of the three events stacked together, using conventional pre-stack depth migration.*

EXAMPLE

In Figure 4 we present several migration results for the model from Figure 2a. Figures 4a, 4b and 4c show the migration result using single Gaussian beams from only one subsurface source. These can be compared to the results from figures 4d, 4e and 4f, which show the results obtained using a conventional SI imaging sequence.

The latter were obtained applying pre-stack depth migration to virtual-source records retrieved for all 41 receiver positions. This is needed to obtain a sufficient destructive interference for suppression of migrated artefacts. Still, the images are quite noisy from migrated artefacts. Contrary to that, the results obtained using the p-evaluation and Gaussian beam migration, needed only 11 virtual-source responses and are much clearer. This comes from using the p-evaluation information to migrate only those reflections that are truly retrieved. The results are defined by the locations of the subsurface source and the receivers: reflectors that are not in stationary phase with the receiver array and the subsurface sources available are not imaged.

Figure 4g is the result of stacking image results from 4a, 4b and 4c. The artefacts from imaging the individual sources are now largely suppressed by destructive interference from the other source images. Figure 4h is the conventional pre-stack migration result of all virtual shot records retrieved from cross-correlating sequentially first and adding consecutively the three subsurface sources.

CONCLUSIONS

We presented a scheme for generating partial images from a limited number of subsurface sources when using seismic interferometry. Our scheme takes the illumination caracteristics of the passive sources into account, and results in suppression of migrated artefacts. If a velocity model is available, the explicit reconstruction of the Green's function is not necessary to image the subsurface. If the passive-source distribution is limited, the scheme produces better results than a conventional interferometric imaging scheme. The contribution from one source alone can describe reflector geometries in the subsurface, and this could be further improved with the eventual addition of other passive sources.